M. A. Ebrahim*, H. A. AbdelHadi, H. M. Mahmoud, E. M. Saied and M. M. Salama

Optimal Design of MPPT Controllers for Grid Connected Photovoltaic Array System

DOI 10.1515/ijeeps-2016-0077

Abstract: Integrating photovoltaic (PV) plants into electric power system exhibits challenges to power system dynamic performance. These challenges stem primarily from the natural characteristics of PV plants, which differ in some respects from the conventional plants. The most significant challenge is how to extract and regulate the maximum power from the sun. This paper presents the optimal design for the most commonly used Maximum Power Point Tracking (MPPT) techniques based on Proportional Integral tuned by Particle Swarm Optimization (PI-PSO). These suggested techniques are, (1) the incremental conductance, (2) perturb and observe, (3) fractional short circuit current and (4) fractional open circuit voltage techniques. This research work provides a comprehensive comparative study with the energy availability ratio from photovoltaic panels. The simulation results proved that the proposed controllers have an impressive tracking response. The system dynamic performance improved greatly using the proposed controllers.

Keywords: photovoltaic, maximum power point tracking techniques, PI controller, particle swarm optimization (PSO), energy availability ratio

1 Introduction

Renewable Energy Resources (RERs) has intensified over the past two decades. Of various alternative energy sources, solar energy is one of the most prominent sources of electrical energy in years to come. The increasing concerns about environmental issues demand the search for more sustainable electrical sources. Solar energy along with wind turbine and fuel cells are possible solutions for environmental energy production [1].

The photovoltaic (PV) generation is one of the most useful applications of RERs. PV sources are used today in many applications such as battery charging, water pumping, home power supply, swimming pool heating system, and satellite systems. They have many advantages like pollution free, silent and directly fed electricity into distribution networks.

Despite all the benefits presented by the PV energy generation, the initial cost for maximum power tracking system implementation is still considered high. Thus, it becomes necessary to use technologies to extract the maximum power from these panels to meet maximum operation efficiency.

The organization of the paper is; Section 1: is the introduction, Section 2: presents a comprehensive description of the system under study, and some ideas about system modeling point of view as it relates to equivalent circuit analysis. Then, Section 3: describes what MPPT entails. Next, the concepts of the most commonly used MPPT techniques were introduced in Section 4. Section 4 presents hybridization between an ideal basic PI controller and MPPT techniques. Section 5 provides Particle Swarm Optimization (PSO) for the optimal parameters tuning. Section 6 concludes the simulation results by discussing how solar irradiance, temperature, current, and voltage relate to maximum power and energy. Section 7 states the main conclusions.

2 System Configuration and modeling

In this section, the proposed system comprises of 100 kW PV array, a dc-dc boost converter, DC-AC converter (inverter) and distribution grid [2, 3]. Figure 1 shows the block diagram of the developed system. Over the past three decades, several types of research studied the mathematical model for the solar cell [4]. The equivalent circuit of the solar cell model consists of photocurrent diode, the parallel resistor (leakage current) and series

***Corresponding author: M. A. Ebrahim,** Department of Electrical Engineering, Faculty of Engineering at Shoubra, Benha University, Cairo, Egypt, E-mail: mohamedahmed_en@yahoo.com
H. A. AbdelHadi, Department of Electrical Engineering, Faculty of Engineering at Shoubra, Benha University, Cairo, Egypt
H. M. Mahmoud, CIGRE, Cairo, Egypt
E. M. Saied, M. M. Salama, Department of Electrical Engineering, Faculty of Engineering at Shoubra, Benha University, Cairo, Egypt

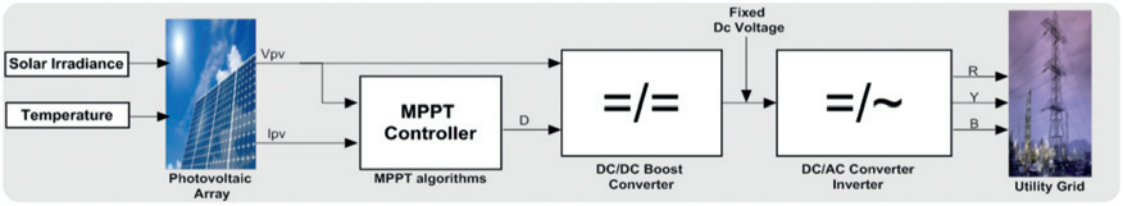

Figure 1: Block diagram for the proposed system.

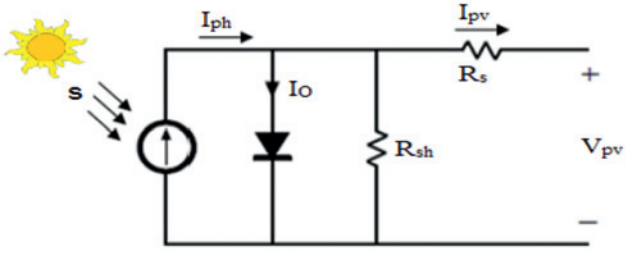

Figure 2: Single diode PV cell equivalent circuit.

resistor as shown in Figure 2. The mathematical model of solar cell is [5, 6].

Photo-current (I_{ph}):

$$I_{ph} = [I_{sc} + K_i(T - T_r)]*G/1000 \quad (1)$$

Where, I_{sc} is PV module short circuit current at 25 °C and 1,000 W/m^2 = 2.55 A and K_i is the short circuit current temperature coefficient at I_{sc} = 0.0017 A/°C. T, T_r are module operating temperature and Reference temperature = 298, respectively and both are in degree Kelvin, and G is the PV module illumination (W/m^2)

Reverse saturation current (I_{rs}):

$$I_{rs} = I_{sc}/[\exp((Q*V_{oc})/(N_s*K*A*T)) - 1] \quad (2)$$

Where, Q is the electron charge = 1.6*10^{-19} C, V_{oc} is the open-circuit voltage (V), N_s is the number of series-connected cells, K is the Boltzmann constant = 1.3805*10^{-23} J/K, and A is the ideality factor = 1.6.

Saturation current (I_o):

$$I_o = I_{rs}*[T/T_r]^3*[\exp(((Q*E_{go})/(B*K))*((1/T_r) - (1/T)))] \quad (3)$$

Where, E_{go}; is the band gap of silicon = 1.1 eV and B is the ideality factor = 1.6

PV output current (I_{pv}):

$$I_{pv} = N_p*I_{ph} - N_s*I_o*[\exp((Q*(V_{pv} + I_{pv}*R_s))/(N_s*A*K*T)) - 1] \quad (4)$$

Where, N_p is the number of parallel-connected cells, V_{pv} is the output voltage of a PV module (V), and R_s is the series resistance of a PV module (Ω).

3 Photovoltaic control system

Bouchouicha and Pandiarajan presented the nonlinear output characteristics of the PV model with different solar irradiance and cell temperature [7, 8]. Furthermore, the maximum power point of the PV module changes continuously due to the unpredictable nature of the solar irradiation. Therefore, a maximum power point tracking technique is required to maintain the output power of the PV module at its maximum power point. Kumar validates the PV model parameters in [4]. Many MPPT tracking methods have been developed and implemented [9]. The main challenge considered by MPPT techniques is how to find automatically the optimal PV array voltage and current to obtain maximum power output PMPP under system uncertainties.

4 MPPT techniques

4.1 Incremental conductance technique

Based on the fact that the Power slope of the PV is null at MPP (dP/dV = 0), Positive in the left and negative in the right as shown in eq. (5). Thus, the incremental conductance (IC) method is employed for achieving MPPT. The IC conditions are

$$\frac{dP}{dV} = \left\{ \begin{array}{l} = 0 \text{ at MPP} \\ > 0 \text{ at the left of MPP} \\ < 0 \text{ at the right of MPP} \end{array} \right\} \quad (5)$$

Where;

$$\frac{dP}{dV} = \frac{d(IV)}{dV} = I + V\frac{dI}{dV} \cong I + V\frac{\Delta I}{\Delta V} \quad (6)$$

$$\frac{\Delta I}{\Delta V} = \begin{cases} =-\frac{I}{V} & \text{at MPP} \\ >-\frac{I}{V} & \text{at the left of MPP} \\ <-\frac{I}{V} & \text{at the right of MPP} \end{cases} \quad (7)$$

Figure 3 shows the use of the instantaneous conductance (I/V) to the incremental conductance to track the MPP. The algorithm decrements or increments duty cycle to track new MPP. The increment size determines how fast the MPP is tracked [9]. In the IC technique, both the instantaneous conductance and the incremental conductance are used to generate an error signal. The possibility of zero division represents a limitation of this technique. In the case of zero division, inserting a tiny number tackled the zero division problem. The objective function of error in this method is

$$\text{Error} = \frac{I}{V} + \frac{dI}{dV} \quad (8)$$

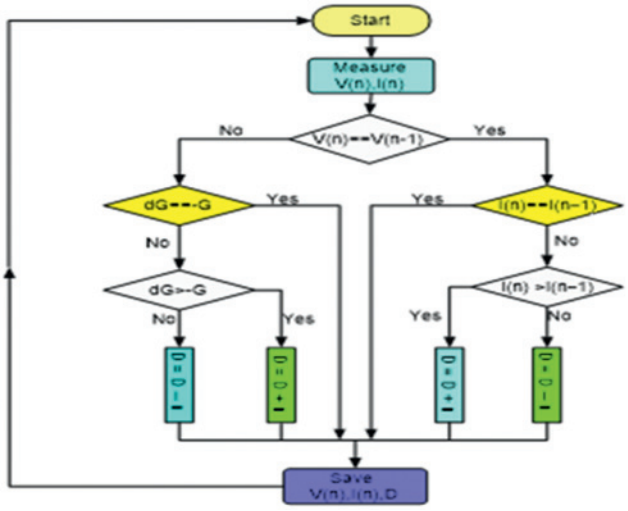

Figure 3: Incremental conductance technique.

The Proportional-Integral (PI) controller can reduce or eliminate this error. Various control systems use PI controller [10, 11]. The continuous form of PI controller, with an input e and output *U*, is presented in eq. (9).

$$U_{PI} = K_p e(t) + K_i \int_0^t e(t)dt \quad (9)$$

– **Proportional gain (K_P):** The proportional gain is responsible for enhancing the overall stability. This term presents multiplication of the system error by adjustable proportional gain K_P.

– **Integral gain (K_i):** the primary control objective is to reduce significantly or eliminate the steady state error. To achieve this goal, authors decided to add integral action to the sum of the instantaneous error over time multiplied by the integral term.

$$integral\ term = K_i \int_0^t e(t)dt \quad (10)$$

4.2 Perturb and observe technique

This section presents a comprehensive explanation for Perturb and observe (P&O) algorithm. P&O involves a perturbation on the duty cycle of the power converter. In this study perturbation of duty cycle of the boost converter is implemented. If the change in power is positive (P) and perturbation is positive, then the next perturbation will be positive. While if the difference in power is negative and the perturbation is positive, therefore the next perturbation will be negative (N) (reversed) [9, 12]. Table 1 summarizes the algorithm. The process is repeated periodically until the MPP is reached [12]. The limitation of this algorithm is that the system oscillates about the MPP. Variable perturbation step size is used to overcome this problem and get smaller towards MPP as shown in Figure 4.

Table 1: P&O algorithm summary.

		Change in Power	
		P	N
Perturbation	P	P	N
	N	N	P

4.3 Fractional open circuit technique

Fractional Open Circuit (OC) depends on the Fractional V_{oc} from the fact that, under varying atmospheric conditions, V_{mpp} is approximately linearly related to V_{oc} of the PV array as shown in Figure 5 [13–15].

$$Vmpp = K1*Voc \quad (11)$$

Where K_1 is dependent on the characteristics of the PV array and has been reported to be between 0.71 and 0.80 [14]. It usually has to be computed empirically determining V_{mpp} and V_{oc} for the specific PV array at different irradiance and temperature levels. Once K_1 is known, V_{mpp} can be calculated using eq. (11). The pilot

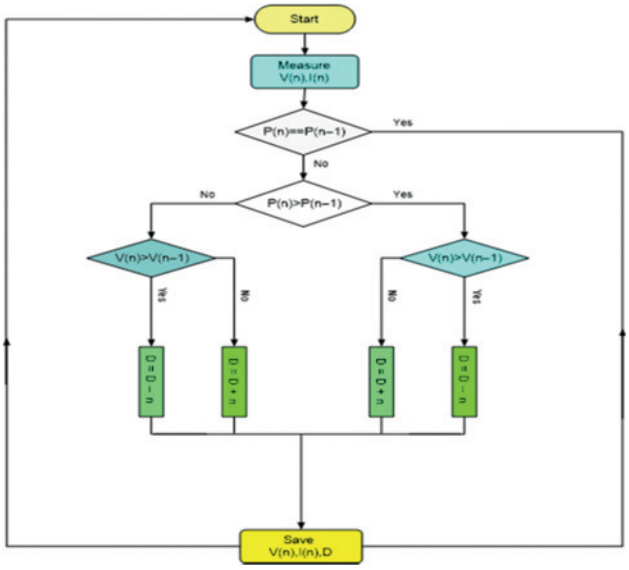

Figure 4: Perturb and observe technique.

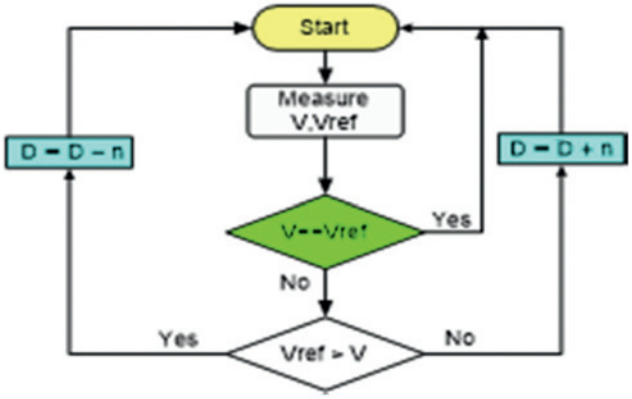

Figure 5: Fractional open circuit algorithm.

cells for measuring V_{oc} had been used to prevent temporary loss of power. These pilot cells must be carefully chosen closely to represent the characteristics of the PV array. The drawback of this technique is that the generated voltage by p-n junction diodes is approximately 75 % of Voc. The objective function of error in this technique can be clarified as follows:

$$\text{Error} = \text{Vref} - K_1 * \text{Vo.c} \tag{12}$$

4.4 Fractional short circuit technique

Based on the fact that, under varying atmospheric conditions, I_{mpp} is approximately linearly related to I_{sc}

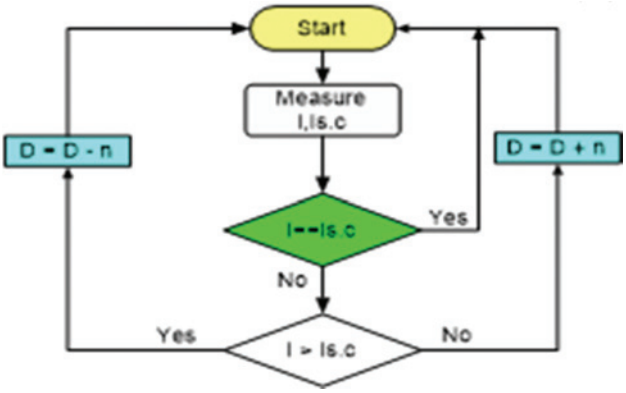

Figure 6: Fractional short circuit technique.

of the PV array as shown in Figure 6 [15]. Fractional Short Circuit (SC) technique is

$$\text{Impp} = K_2 * I_{s.c} \tag{13}$$

Where K_2 has to be determined according to the PV array in use. Just like in the fractional V_{oc} technique, the constant K_2 is found to be between 0.78 and 0.92 [16]. The objective function of error in this technique is

$$\text{Error} = I_{ref} - K_2 * I_{s.c} \tag{14}$$

5 Particle swarm optimization technique

PSO is a population-based stochastic optimization algorithm that emulates from the behavior of birds flocking and fish schooling that doesn't have any leader in their group or swarms [17]. PSO has two populations' p_{bests} and current positions; this allows greater diversity and exploration over a single population. Also, the momentum effects on particle movement can allow faster convergence. It is developed through simulation of birds flocking in two-dimension space [18, 19]. Figure 7 presents general flowchart of PSO. The particles flew through the search space by updating the position of the i^{th} particle at time step according to Equation (15)

$$x_i(t+1) = x_i(t) + v_i(t+1) \tag{15}$$

The velocity updates are

$$\begin{aligned} V_i(t+1) = \sigma\ & v_i(t) + c_1\ \text{rand}_1\ x\ (\text{pbest}_i - x_i(t) \\ & + c_2\ \text{rand}_2\ x(\text{gbest} - x_i(t)) \end{aligned} \tag{16}$$

Where, $x_i(t)$, $V_i(t\ +\ 1)$, and are the vector of the current position, the vector of current velocity, and the inertia

weighting function respectively. The inertia weighting function is a linearly decreasing function [20, 21]. c, rand, p_{besti}, and g_{besti} are the acceleration constant, the random number on the interval [0, 1], the personal best of particle and Global best (best of p_{best} of the group) respectively.

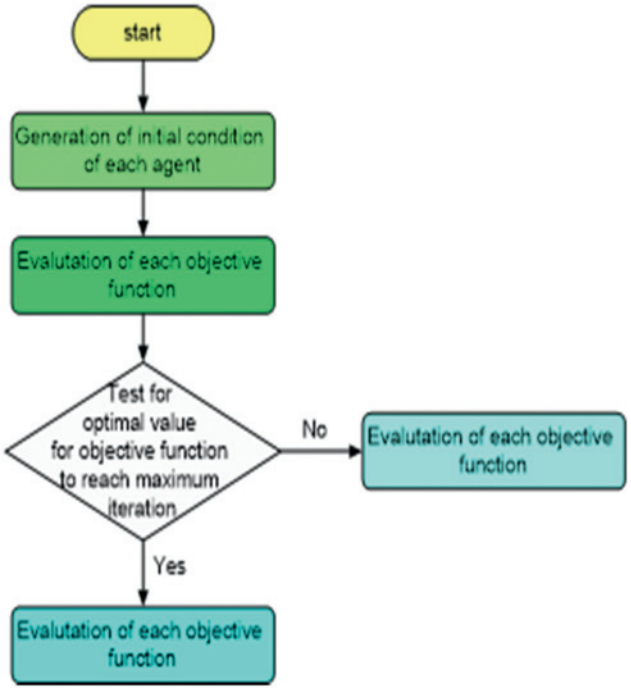

Figure 7: A general flowchart of PSO.

6 Results and discussion

Figure 8 shows the I-V and P-V output characteristics for the PV model. The output power and current of PV module depend on the solar irradiance and temperature, and as well cell's terminal operating voltage. From Figure 8, like solar irradiance increases as the maximum power output and short circuit current increases. In Figure 9, the step-up DC/DC boost converter increases the normal voltage of PV from 272 VDC at full power to 500 VDC.

Figures 10 and 12 present the proposed system tested under two cases with different irradiance pattern. After implementing the IC technique, P&O technique, SC and OC techniques on both two cases. It is evident that the output power obtained from PV after applying IC technique performs best results than any other techniques as shown in Table 2. Figures 11 and 13 present the dynamic and transient responses of the four techniques.

Table 3 shows optimal values of gains K_P and K_i obtained from PSO. Table 3 indicates that SC has the lowest overshoot compared to IC and OC. The IC can reach MPP faster than both SC and OC as shown in Table 3. Table 3 reveals that the IC has better tracking response; however the rise time is nearly constant in all techniques. Figures 14 and 15 show the grid voltage and current.

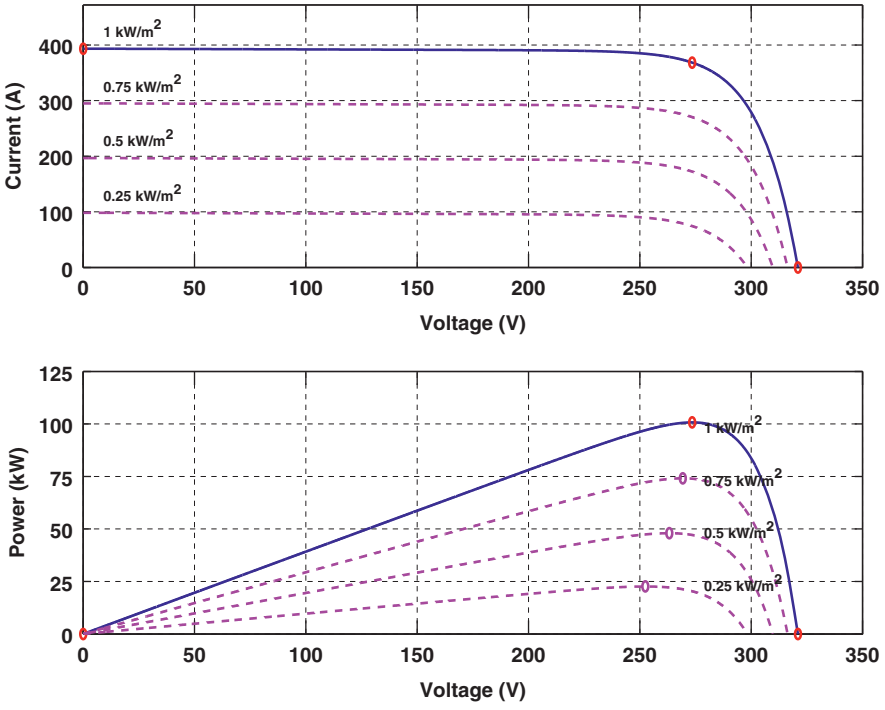

Figure 8: I-V and P-V characteristic of PV array.

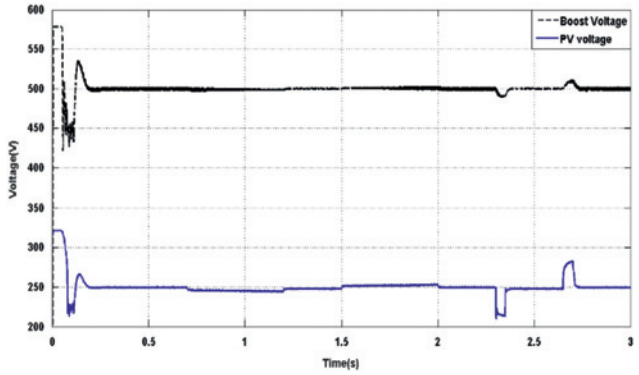

Figure 9: Output voltage of PV and boost converter.

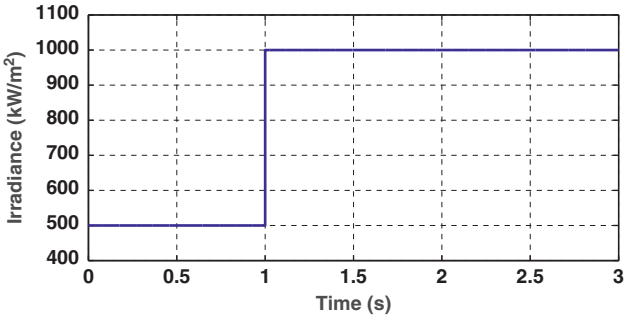

Figure 10: Solar irradiance pattern for case study 1.

Table 2: Available power shared for each MPPT technique.

Case Study	IC	P&O	SC	OC
				Power Shared (kW)
1	99.1	94.3	98.2	93.9
2	99.1	94.4	94.4	96.5

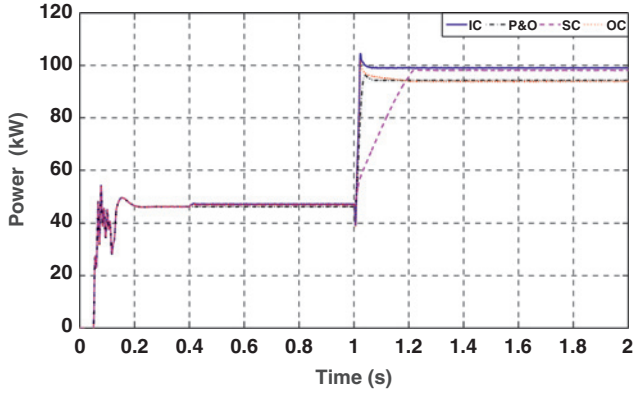

Figure 11: Dynamic response of PV output power with MPPT controllers.

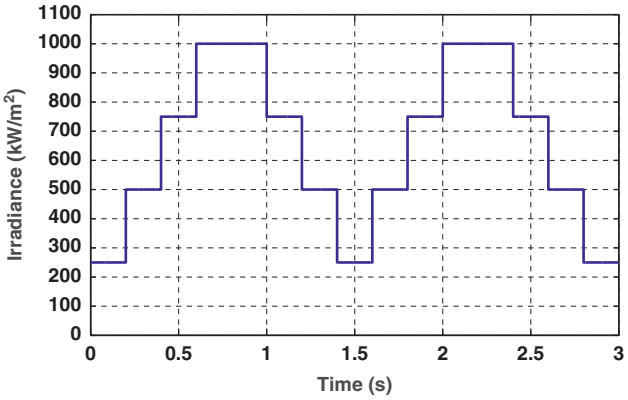

Figure 12: Solar irradiance pattern for case study 2.

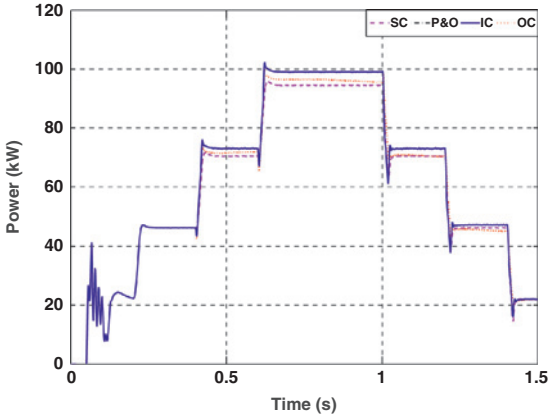

Figure 13: Transient behavior of PV output power.

Table 3: Optimal values of Kp and Ki obtained by PSO.

	Incremental Conductance	Fractional Open Circuit	Fractional Short Circuit
K_p	17.736	14.947	4.9089
K_i	32.51	30.014	7.7415
Rise time (t_r)μ sec.	0.967	0.967	1.105
Settling time (t_s)μ sec.	1.027	1.043	1.197
Maximum Overshoot(M_p)	5.461	8.369	0.234

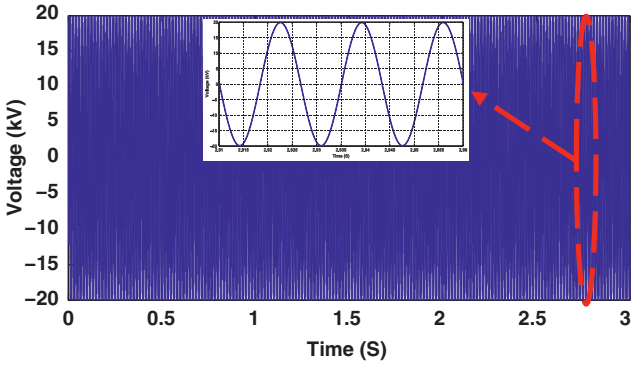

Figure 14: Grid output voltage.

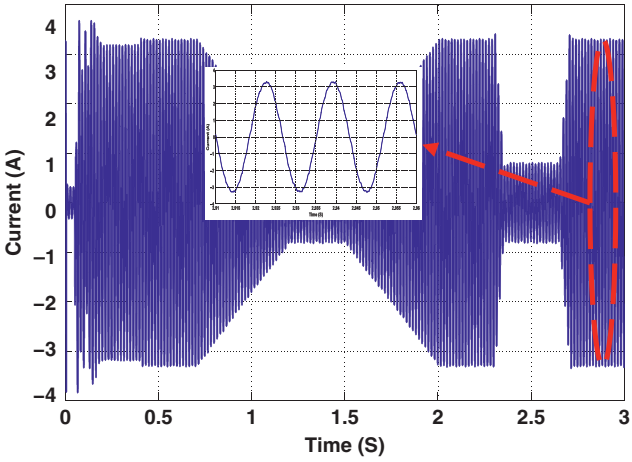

Figure 15: Grid output current.

7 Conclusion

In this paper, a new effective control method integrating PSO-based PI was introduced. This research article demonstrates that PSO can solve searching the controller parameters more efficiently than conventional ones. Modeling of the proposed system was performed using MATLAB/SIMULINK software package. The simulation was conducted to cover the full range of operating conditions and severe disturbances. It is evident from simulation results that the Incremental conductance technique performs best results in both two cases of study (different irradiance pattern) as compared with the other techniques of MPPT with availability power ratio.

Acknowledgement: The authors acknowledge the support of the Scientific and Technology Development Fund (STDF) and Benha University from Egypt. Also, special thanks to the Institute of Research and Development (IRD) and the University of Technology in Belfort (UTBM) from France.

References

1. Natsheh E, Albarbar A, Yazdani J. Modeling and control for smart grid integration of solar/wind energy conversion system. 2nd IEEE PES International Conference on Innovative Smart Grid Technologies 2011;1:1–8.
2. Zhou Y, Huang W, Zhao P, Zhao J. A Transformerless grid- connected photovoltaic system based on the coupled inductor single stage boost three phase inverter. IEEE Trans 2013;29:1041–6.
3. Stallon SD, Kumar KV, Kumar SS, Baby J. Simulation of High step-up DC-DC converter for photovoltaic module application using MATLAB/SIMULINK. Intell Syst Appl 2013;5:72–82.
4. Kumar R, Muralidharan R. Mathematical modeling simulation and validation of photovoltaic cells. Int J Res Eng Technol 2014;3:170–4.
5. Pranahita BS, Kumar AS, Babu APA. Study on modeling and simulation of photovoltaic cells. Int J Res Eng Technol 2014;3:101–8.
6. Jakhrani AQ, Samo SR, Kamboh SA, Labadin J, Rigit RH. An improved mathematical model for computing power output of solar photovoltaic modules. Int J Photo Energy 2014;2014:1–9.
7. Bouchouicha K, Nahman B, Chenni R, Aoun N. Evaluation and validation of equivalent five parameters model performance for photovoltaic panels using only reference data. Energy Power Eng 2014;6:235–45.
8. Pandiarajan N, Muthu R. Mathematical Modeling of photovoltaic module with Simulink. Int Conf Electr Energy Syst 2011;6:03–05:314–19.
9. Esram T, Chapman PL. Comparison of photovoltaic array maximum power point tracking techniques. IEEE Trans Energy Convers 2007;22:439–49.
10. Ebrahim MA, Jagatheesan K, Anand B. Stochastic particle swarm optimization for tuning of PID controller in load frequency control of single area reheat thermal power system. Int J Electr Power Eng 2014;8:33–44.
11. Ebrahim MA, Mousa ME, Hassan MA. Stabilizing and swinging-up the inverted pendulum using PI and PID controllers based on reduced linear quadratic regulator tuned by PSO. Int J Syst Dyn Appl 2015;4:52–69.
12. Elgendy MA, Zahawi B, Alkinson DJ. Assessment of perturb and observe MPPT algorithms implementation techniques for PV Pumping applications. IEEE Trans Sustain Energy 2012;3:21–33.
13. Ahmad J. A fractional open circuit voltage based maximum power point tracker for photovoltaic arrays. Int Conf Software Technol Eng 2010;1:247–50.
14. Games MA, Galotto L, Sampaio LP, Melo G, Canesin CA. Evaluation of the Main MPPT Techniques for photovoltaic applications. IEEE Trans Ind Electron 2013;60:1156–67.
15. Onat N. Recent developments in maximum power point tracking technologies for photovoltaic systems. Int J Photo Energy 2010;2010:2–11.
16. Canesin CA, Melo GA, Sampaio LP, Brito AG. Comparative Analysis of MPPT techniques for PV applications. 3rd international conference on clean electrical power renewable energy resources, 2011;2011:99–104.
17. Ebrahim MA, El-Metwally KA, Bendary FM, Mansour MW. Optimization of proportional integral- differential controller for wind power plant using particle swarm optimization technique. Int J Electr Power Eng 2012;6:32–7.
18. Sarvi M, Ahmadi S, Abdi SA. PSO-based maximum power point tracking for photovoltaic systems under environmental and partially shaded conditions. Photovoltaics Res Appl 2015;23:201–14.
19. Priyadarshini J, Karthiga J. Survey on various MPPT techniques on WECS (DFIG). Int J Adv Inf Sci Technol 2014;23:144–48.
20. Ebrahim MA, El-Metwally KA, Bendary FM, Mansour WM, Ramadan SH, Ortega R, et al. Optimization of proportional integral-differential controller for wind power plant using particle swarm optimization technique. Int J Emerg Technol Sci Eng 2011;2011:1–6.
21. Ebrahim MA, Mostafa EH, Gawish AS, Bendary FM. Design of decentralized load frequency based-PID controller using stochastic particle swarm optimization technique. Int Conf Electr Power Energy Convers Syst Nov 2009;2009:1–6.